Int. J. Solids Structures, 1978, Vol. 14, pp. 305–318. Pergamon Press. Printed in Great Britain

AXISYMMETRIC STRESSES IN TRANSVERSELY ISOTROPIC FINITE CYLINDERS†

CHIRUVAI P. VENDHAN and ROBERT R. ARCHER‡
Department of Civil Engineering, University of Massachusetts, Amherst, MA 01003, U.S.A.

(*Received* 11 *July* 1977; *received for publication* 1 *December* 1977)

Abstract—The elastostatic analysis of transversely isotropic finite cylinders with stress-free lateral surfaces is considered using the formulation in terms of a displacement potential. Solution in the form of the eigenfunction expansion where each of the eigen-functions satisfies the lateral boundary conditions is obtained. The end conditions are satisfied by means of the general orthogonality relations for the radial eigenfunctions. The orthogonality technique gives closed-form expressions for the Fourier–Bessel coefficients for certain types of mixed end conditions. For other cases the technique leads to an infinite set of linear equations. The convergence of these equations are examined and solutions are obtained by suitable truncation. Both stress and displacement end conditions are considered and numerical results for two types of transversely isotropic materials are presented.

NOTATION

$(a, \bar{\mu}, b, \bar{a}, \mu)$	TI material constants defined in eqn (4)
c_1 and c_2	separation constants in the differential eqn (1)
E_m and E_w	material parameters used for normalization; see Table 1—$\bar{E}_m = E_m/10^6$; $\bar{E}_w = E_w/10^6$
F_j	radial eigenfunction
J_n	Bessel function of the first kind
K	c_2/c_1
$2l$	length of the cylinder
m	number of eigenfunctions in the expansion
$(\hat{r}, \hat{z})$	radial and axial coordinates, where $r = \hat{r}/r_0$ and $z = \hat{z}/r_0$
r_0	radius of the cylinder
$(\hat{u}, \hat{w})$	displacements in the $(\hat{r}, \hat{z})$ system where $u = \hat{u}/r_0$ and $w = \hat{w}/r_0$
z_0	l/r_0
$(\epsilon_{rr}, \gamma_{rz})$	normal and shear strains
ϕ	displacement potential
λ_j	eigenvalue, with $\tilde{\lambda}_j = \lambda_j/c_1$
ρ	unit weight of the cylinder
(σ_{rr}, τ_{rz})	normal and shear stresses
$(\sigma_k, w_k, \tau_k, u_k)$	eigenfunctions defined in eqn (20)
$(\bar{\sigma}, \bar{\sigma}')$	end conditions defined in eqn (19)
θ	circumferential coordinate

INTRODUCTION

The elastostatic analysis of cylinders under end loading has been the subject of many investigations[1–4]. Earlier researchers were confronted by computational difficulties associated with arbitrary end conditions, singularities under certain end conditions and lack of suitable orthogonality relations for the radial eigenfunctions. The solution of a semi-infinite cylinder, like a semi-infinite strip, can be sought as a combination of eigensolutions, which decay axially, as well as a nondecaying elementary solution. The technique of eigenfunction expansion with the end conditions being satisfied using a least-square procedure is convenient with a digital computer[5]. Little and Childs[6] have developed biorthogonality relations for the radial eigenfunctions of an isotropic cylinder which have been used in the solution of several end problems[3]. Fama[7] derived more general orthogonality relations for an isotropic cylinder. Following Fama, Byrnes and Archer[8] presented the orthogonality conditions for a transversely isotropic (TI) cylinder. Although these relations have been used in the solution of a few isotropic problems, their computational features have not been studied especially for TI cylinders.

The solution of finite cylinders is closely related to the semi-infinite case. Pickett[9] analyzed an isotropic cylinder under axial compression using a multiple Fourier–Bessel Series

†Paper presented at the Sixth Canadian Congress of Applied Mechanics, University of British Columbia, Vancouver, B.C., Canada, 30 May–3 June 1977.

‡The work of both the authors was supported in part by NSF Grant ENG-74-02428.

Solution. Moghe and Neff[10] used a similar analysis for a constrained elastomeric cylinder under end compression. Power and Childs[11] considered an isotropic finite cylinder and obtained solutions by means of the biorthogonal eigenfunction expansion developed for a semi-infinite case[6]. Mitra[12] considered a TI finite cylinder, but his solution does not admit arbitrary end conditions. References to the analysis of finite cylinders using numerical techniques may be found in[2, 11]. The present paper considers the exact analysis of axisymmetric, TI finite cylinders with arbitrary end conditions using the general orthogonality relations[7, 8].

A linear elasticity formulation in terms of the displacement potential due to Eubanks and Sternberg[5, 13] is adopted. The solution for a finite TI cylinder with stress-free lateral surface is constructed from the radial eigenfunctions of the semi-infinite case and a zero-eigenvalue solution. The coefficients of the eigenfunction expansion are evaluated by means of the general orthogonality conditions. The orthogonality technique yields closed form solutions for certain types of mixed end conditions. In other cases the technique leads to an infinite set of linear equations which can be solved after suitable truncation. The conditions for the convergence of the solution of these equations are briefly examined. A few typical combinations of end conditions are studied, and solutions by the least-square method are obtained for comparison. For a short cylinder with only axial loading, the limiting case of a plane stress model[14] is compared with the exact analysis.

2. ANALYSIS

Consider a circular cylinder in the region $\hat{r}\epsilon[0, r_0]$ and $\hat{z}\epsilon[\pm l]$ where r_0 is the radius and $2l$ is the length of the cylinder. The linear elastostatic equations of an axisymmetric TI cylinder in the absence of body forces can be written as[5, 13]

$$\left(\frac{\partial^2}{\partial\hat{r}^2}+\frac{1}{\hat{r}}\frac{\partial}{\partial\hat{r}}+c_1^2\frac{\partial^2}{\partial\hat{z}^2}\right)\left(\frac{\partial^2}{\partial\hat{r}^2}+\frac{1}{\hat{r}}\frac{\partial}{\partial\hat{r}}+c_2^2\frac{\partial^2}{\partial\hat{z}^2}\right)\phi=0 \tag{1}$$

where the displacement potential ϕ is defined as

$$\hat{u}=-(b+\mu)\phi_{,\hat{r}\hat{z}}$$
$$\hat{w}=a\left[\phi_{,\hat{r}\hat{r}}+\frac{1}{\hat{r}}\phi_{,\hat{r}}\right]+\mu\phi_{,\hat{z}\hat{z}} \tag{2}$$

with $(.)$ denoting partial differentiation. c_1^2 and c_2^2 are the roots of the equation

$$x^2+[(b^2+2b\mu-a\bar{a})/a\mu]x+\bar{a}/a=0 \tag{3}$$

where the stress–strain relations are

$$\begin{Bmatrix}\sigma_{rr}\\ \sigma_{\theta\theta}\\ \sigma_{zz}\\ \tau_{rz}\end{Bmatrix}=\begin{bmatrix}a & (a-2\bar{\mu}) & b & 0\\ & a & b & 0\\ \text{Sym.} & & \bar{a} & 0\\ & & & \mu\end{bmatrix}\begin{Bmatrix}\epsilon_{rr}\\ \epsilon_{\theta\theta}\\ \epsilon_{zz}\\ \gamma_{rz}\end{Bmatrix}. \tag{4}$$

It can be shown that the form of the solution of eqn (1) for a TI cylinder is

$$\phi=\phi_1+\phi_2 \tag{5}$$

where ϕ_i are harmonic functions. For a semi-infinite cylinder in the region $\hat{r}\epsilon[0, r_0]$ and $\hat{z}\epsilon[-l, \infty]$ the decaying solution may be taken as an aggregate of the eigenfunctions:

$$\phi'=\sum_j A_j\,e^{-\tilde{\lambda}_j z}[J_0(\lambda_j r)+B_j J_0(K\lambda_j r)] \tag{6}$$

where $r=\hat{r}/r_0$, $z=\hat{z}/r_0$, $K=c_2/c_1$, $\tilde{\lambda}_j=\lambda_j/c_1$, and λ_j are nonzero eigenvalues. A_j are constants

evaluated from the boundary conditions at the end $\hat{z} = -l$ and B_j are obtained from the eigenvalue problem. The expressions for stresses and displacements can conveniently be written as

$$\sigma_{rr} = \sum_j \sum_{i=1,2} A_j\{\mu(ac_i^2 + b)R_{ij}Z_{j,zzz} + 2\bar{\mu}(b+\mu)R_{ij,r}Z_{j,z}/r\}$$

$$\sigma_{\theta\theta} = \sum_j \sum_{i=1,2} A_j\{[\{-2\bar{\mu}(b+\mu) + a\mu\}c_i^2 + b\mu]R_{ij}Z_{j,zzz} - 2\bar{\mu}(b+\mu)R_{ij,r}Z_{j,z}/r\}$$

$$\sigma_{zz} = \sum_j \sum_{i=1,2} A_j\{\bar{a}\mu - [a\bar{a} - b(b+\mu)]c_i^2\}R_{ij}Z_{j,zzz} \tag{7}$$

$$\tau_{rz} = \sum_j \sum_{i=1,2} A_j\{-\mu(ac_i^2 + b)\}R_{ij,r}Z_{j,zz}$$

$$u = \sum_j \sum_{i=1,2} A_j\{-(b+\mu)\}R_{ij,r}Z_{j,z}$$

$$w = \sum_j \sum_{i=1,2} A_j\{\mu - ac_i^2\}R_{ij}Z_{j,zz}$$

where

$$R_{1j} = J_0(\lambda_j r), \qquad R_{2j} = B_j J_0(K\lambda_j r), \qquad Z_j = e^{-\tilde{\lambda}_j z} \tag{8}$$

with $u = \hat{u}/r_0$, $w = \hat{w}/r_0$ and $z_0 = l/r_0$. For a cylinder with zero stresses on the lateral surface, which is of concern in the present investigation, the boundary conditions may be written as

$$\begin{bmatrix} d_{11} & d_{12} \\ d_{21} & d_{22} \end{bmatrix} \begin{Bmatrix} A_j \\ \tilde{A}_j \end{Bmatrix} = 0 \tag{9}$$

where

$$d_{1k} = -\mu(ac_k^2 + b)J_0(\beta_k)\tilde{\lambda}_j^3 + 2c_k\bar{\mu}(b+\mu)J_1(\beta_k)\tilde{\lambda}_j^2 \tag{10}$$

$$d_{2k} = c_k\mu(ac_k^2 + b)J_1(\beta_k)\tilde{\lambda}_j^3$$

$$\tilde{A}_j = A_jB_j, \quad \beta_1 = \lambda_j \quad \text{and} \quad \beta_2 = K\lambda_j. \tag{11}$$

The condition for the nontrivial solution of eqn (9) yields an equation of the form $G(\lambda) = 0$ with roots λ_j. Then eqn (9) can be solved for B_j. The eigenspectrum lying in the right half of the complex plane yields decaying solutions. By an analogous procedure it follows that the decaying solution for a semi-infinite cylinder in the region $\hat{r}\epsilon[0, r_0]$ and $\hat{z}\epsilon[l, -\infty]$ is given by

$$\phi'' = \sum_j A_j' e^{\tilde{\lambda}_j z}[J_0(\lambda_j r) + B_j J_0(K\lambda_j r)] \tag{12}$$

where λ_j obviously lies in the right half of the complex plane, and A_j' depends on the boundary conditions at $\hat{z} = l$.

It is easy to show that the complete solution to a finite cylinder with no body forces can be written as a combination of the above eigenfunction expansions for the two semi-infinite cases:

$$\phi = \phi_0 + \sum_j [(A_{1j} e^{\tilde{\lambda}_j z} + A_{2j} e^{-\tilde{\lambda}_j z})/e^{\tilde{\lambda}_j z_0}]F_j(\lambda_j, r) \tag{13}$$

where ϕ_0 is the zero-eigenvalue solution, discussed subsequently, and F_j is the eigenfunction given by

$$F_j(\lambda_j, r) = \{J_0(\lambda_j r) + B_j J_0(K\lambda_j r)\}. \tag{14}$$

A_{1j} and A_{2j} are constants to be evaluated from the conditions at $z = \pm z_0$. The expressions for stresses and displacements are given by eqns (7) where

$$Z_j = (A_{1j}\, e^{\lambda_j \hat{r}^2} + A_{2j}\, e^{-\lambda_j \hat{r}^2})/e^{\lambda_j z_0}. \tag{15}$$

Zero-eigenvalue solution:

The solution of eqn (1) corresponding to $\lambda_0 = 0$ assumes the form

$$\phi_0 = (a_1 z + a_2)r^2 + a_3 z^3 + a_4 z^2 + a_5 z + a_6. \tag{16}$$

Deleting the terms which do not affect the displacements or stresses,

$$\phi_0 = a_1 z r^2 + a_3 z^3 + a_4 z^2. \tag{17}$$

The last term in eqn (17) as well as the a_2-term in eqn (16) represent rigid body displacements along z. It is enough to retain one of them. Upon satisfying the zero-stress condition at $\hat{r} = r_0$ one has

$$\phi_0 = a_1 z \left[r^2 - \frac{2\{\bar{\mu}(b+\mu) - a\mu\}}{3b\mu} z^2 \right] + a_4 z^2. \tag{18}$$

The first term in eqn (18) represents a uniform axial stress state in the cylinder.

3. SOLUTIONS FOR ARBITRARY END CONDITIONS

The uniform normal stress distribution on the ends directly determines a_1 in eqn (18). The constants A_{1j} and A_{2j} in the eigenfunction expansion are evaluated from the self-equilibrated end conditions. A convenient method of satisfying these conditions approximately is by means of a least-square procedure. The biorthogonality technique developed by Little and Childs[6] can also be used to evaluate the coefficients of the eigenfunction expansion. Power and Childs[11] adopted this method for finite isotropic cylinders. Alternatively, the general orthogonality relations developed by Fama[7] for an isotropic cylinder and later extended to a TI case by Byrnes and Archer[8] provide an elegant method of determining the Fourier–Bessel coefficients. The features of such an analysis for a TI finite cylinder are studied in this paper. The various combinations of end conditions considered are

$$\left.\begin{array}{lll} \text{(i)} & \sigma_{zz}(r, z) = \bar{\sigma}(r), & u(r, z) = \bar{u}(r) \\ \text{(ii)} & w(r, z) = \bar{w}(r), & \tau_{rz}(r, z) = \bar{\tau}(r) \\ \text{(iii)} & \sigma_{zz}(r, z) = \bar{\sigma}(r), & \tau_{rz}(r, z) = \bar{\tau}(r) \\ \text{(iv)} & w(r, z) = \bar{w}(r), & u(r, z) = \bar{u}(r) \end{array}\right\} \text{at} \quad z = z_0. \tag{19}$$

The quantities at the end $z = -z_0$ are distinguished by a prime, e.g. $\bar{\sigma}'$. Solutions are obtained by means of the orthogonality technique, and a few results for comparison are obtained using the least-square integral technique as well as a least-square point matching technique.

3.1 *Orthogonality technique*

The orthogonality relations among the radial eigenfunctions of a TI cylinder with zero stresses at $r = 1$ is given by[7, 8].

$$\int_0^1 (\sigma_j w_k - \tau_k u_j) r \, dr = 0 \qquad k \neq j \tag{20}$$

where $(\sigma_j, w_j, \tau_j, u_j)$ are the radial eigenfunctions associated with $(\sigma_{zz}, w, \tau_{rz}, u)$. Let the

Fourier–Bessel expansion for the solution of a finite cylinder be

$$\begin{Bmatrix} \sigma_{zz} \\ w \\ \tau_{rz} \\ u \end{Bmatrix} = \sum_{j>0} \begin{Bmatrix} [(A_{1j}\,e^{\bar{\lambda}_j z} - A_{2j}\,e^{-\bar{\lambda}_j z})/e^{\bar{\lambda}_j z_0}]\sigma_j \\ [(A_{1j}\,e^{\bar{\lambda}_j z} + A_{2j}\,e^{-\bar{\lambda}_j z})/e^{\bar{\lambda}_j z_0}]w_j \\ [(A_{1j}\,e^{\bar{\lambda}_j z} + A_{2j}\,e^{-\bar{\lambda}_j z})/e^{\bar{\lambda}_j z_0}]\tau_j \\ [(A_{1j}\,e^{\bar{\lambda}_j z} - A_{2j}\,e^{-\bar{\lambda}_j z})/e^{\bar{\lambda}_j z_0}]u_j \end{Bmatrix} + A_0 \begin{Bmatrix} \sigma_0 \\ zw_0 \\ \tau_0 \\ u_0 \end{Bmatrix} \tag{21}$$

where the second vector is the zero-eigenvalue solution. Let $\sigma_{zz} = \bar{\sigma}$ and $u = \bar{u}$ be prescribed at $z = z_0$. Then, upon using the orthogonality relation (20) in the eigenfunction expansion one gets

$$[A_{1k} - A_{2k}\,e^{-2\bar{\lambda}_k z_0}] = \frac{1}{C_k}\int_0^1 (\bar{\sigma}w_k - \bar{u}\tau_k)r\,dr \tag{22}$$

where

$$C_k = \int_0^1 (\sigma_k w_k - \tau_k u_k)r\,dr. \tag{23}$$

Let $w = \bar{w}$ and $\tau_{rz} = \bar{\tau}$ be prescribed at $z = z_0$. Then one has instead of eqn (22)

$$[A_{1k} + A_{2k}\,e^{-2\bar{\lambda}_k z_0}] = \frac{1}{C_k}\int_0^1 (\bar{w}\sigma_k - \bar{\tau}u_k)r\,dr. \tag{24}$$

A set of equations similar to eqns (22) and (24) can be obtained from the end conditions at $z = -z_0$.

Now, let $(\bar{\sigma}, \bar{u})$ at $z = z_0$ and $(\bar{\sigma}', \bar{u}')$ at $z = -z_0$ be the prescribed end conditions. Then, using the basic eqns (22) and (24) and their counterparts associated with the end conditions at $z = -z_0$,

$$\begin{aligned} A_{1k} &= \frac{1}{\Delta_1 C_k}\int_0^1 [(\bar{\sigma}w_k - \bar{u}\tau_k) - e^{-2\bar{\lambda}_k z_0}(\bar{\sigma}'w_k - \bar{u}'\tau_k)]r\,dr \\ A_{2k} &= \frac{1}{\Delta_1 C_k}\int_0^1 [-(\bar{\sigma}'w_k - \bar{u}'\tau_k) + e^{-2\bar{\lambda}_k z_0}(\bar{\sigma}w_k - \bar{u}\tau_k)]r\,dr \end{aligned} \tag{25}$$

where

$$\Delta_1 = (1 - e^{-4\bar{\lambda}_k z_0}), \qquad k > 0.$$

If $(\bar{w}, \bar{\tau})$ at $z = z_0$ and $(\bar{w}', \bar{\tau}')$ at $z = -z_0$ are the end conditions, the orthogonality technique leads to the following equations.

$$\begin{aligned} A_{1k} &= \frac{1}{C_k\Delta_1}\int_0^1 [(\bar{w}\sigma_k - \bar{\tau}u_k) - e^{-2\bar{\lambda}_k z_0}(\bar{w}'\sigma_k - \bar{\tau}'u_k)]r\,dr \\ A_{2k} &= \frac{1}{C_k\Delta_1}\int_0^1 [(\bar{w}'\sigma_k - \bar{\tau}'u_k) - e^{-2\bar{\lambda}_k z_0}(\bar{w}\sigma_k - \bar{\tau}u_k)]r\,dr. \end{aligned} \tag{26}$$

Thus it is seen that for the two types of mixed end conditions considered above one gets closed-form expressions for the Fourier–Bessel coefficients. If $(\bar{\sigma}, \bar{\tau})$ or $(\bar{u}, \bar{w})$ are the end conditions, the orthogonality technique leads to, as in the case of semi-infiite cylinders, an infinite set of linear equations involving A_{1k} and A_{2k}. For example when $(\bar{\sigma}, \bar{\tau})$ at $z = z_0$ and $(\bar{\sigma}', \bar{\tau}')$ at $z = -z_0$ are given, it can be shown that

$$\begin{aligned} A_{1k} = \frac{1}{2C_k E_{kk}}\int_0^1 \{&(\bar{\sigma}w_k - \bar{\tau}u_k) - e^{-2\bar{\lambda}_k z_0}(\bar{\sigma}'w_k - \bar{\tau}'u_k) \\ &+ \sum_{j>0} A_{1j}E_{kj}(w_j\sigma_k - u_j\tau_k) + \sum_{j>0} A_{2j}G_{kj}(w_j\sigma_k + u_j\tau_k)\}r\,dr \end{aligned}$$

$$A_{2k} = \frac{1}{2C_kE_{kk}} \int_0^1 \left\{ -(\bar{\sigma}' w_k + \bar{\tau}' u_k) + e^{-2\bar{\lambda}_k z_0}(\bar{\sigma} w_k + \bar{\tau} u_k) \right. \tag{27}$$

$$\left. + \sum_{j>0} A_{1j} G_{kj}(w_j \sigma_k + u_j \tau_k) + \sum_{j>0} A_{2j} E_{kj}(w_j \sigma_k - u_j \tau_k) \right\} r \, dr$$

where

$$E_{kj} = [1 - e^{-2(\bar{\lambda}_k + \bar{\lambda}_j) z_0}], \qquad G_{kj} = [e^{-2\bar{\lambda}_j z_0} - e^{-2\bar{\lambda}_k z_0}]; \quad k > 0. \tag{28}$$

In the above case the zero-eigenfunction uncouples from nonzero-eigenfunctions. A similar set of equations follow for the end conditions ($\bar{w}$, $\bar{u}$) at $z = z_0$ and ($\bar{w}'$, $\bar{u}'$) at $z = -z_0$:

$$A_{1k} = \frac{1}{2C_kE_{kk}} \int_0^1 \left\{ (\bar{w}\sigma_k - \bar{u}\tau_k) - e^{-2\bar{\lambda}_k z_0}(\bar{w}'\sigma_k - \bar{u}'\tau_k) \right.$$

$$\left. + \sum_i A_{1j} E_{kj}(\sigma_j w_k - \tau_j u_k) - \sum_j A_{2j} G_{kj}(\sigma_j w_k + \tau_j u_k) \right\} r \, dr \tag{29}$$

$$A_{2k} = \frac{1}{2C_kE_{kk}} \int_0^1 \left\{ (\bar{w}'\sigma_k + \bar{u}'\tau_k) - e^{-2\bar{\lambda}_k z_0}(\bar{w}\sigma_k + \bar{u}\tau_k) \right.$$

$$\left. - \sum_j A_{1j} G_{kj}(\sigma_j w_k + \tau_j u_k) + \Sigma A_{2j} E_{kj}(\sigma_j w_k - \tau_j u_k) \right\} r \, dr \tag{30}$$

where $k > 0$. For $k = 0$ the relevant equation can be directly obtained from eqns (20) and (21). Note that $E_{kj} \to 1$ and $G_{kj} \to 0$ for large values of k and j as well as z_0. The two ends of the cylinder obviously have very little mutual influence as z_0 increases. Equations similar to (27) for any given combination of end conditions can be derived from the basic eqns (22)–(24). Equations (25) or (27) may be rearranged in the following form for a given number of eigenfunctions m.

$$[S_{pq}] \begin{Bmatrix} A_{1k} \\ A_{2k} \end{Bmatrix} = \{P\} \tag{30}$$

where $p, q = 1, \ldots, 2m$, and $k = 1, \ldots, m$; $\{P\}$ is derived from the end conditions. The convergence of the sequence of solutions of eqn (30) as $m \to \infty$ is discussed in Appendix 1.

4. COMPUTATIONAL DETAILS

The two major steps in the numerical evaluation of the coefficients of the eigenfunction expansion are (i) computation of the eigenvalues λ_j associated with eqn (9); and (ii) computation of the coefficients A_{1j} and A_{2j} for a given set of end conditions. The approximate locations of the roots λ_j of the transcendental equation associated with eqn (9) are obtained by using the computer printer to print the quadrant locations of the function at a grid of points in the λ-plane. The approximate roots are then refined by a Newton–Raphson iteration. The complex Bessel functions $J_0(x)$ and $J_1(x)$ are computed accurate up to seven digits using the infinite series for values of $|x| \leq 10$ and the Hankel asymptotic expansions for $|x| > 10$. The elements of the matrix $[S_{pq}]$ ion eqn (30) appear as a linear combination of the following integrals:

$$\int_0^1 J_0(p_1 r) J_0(p_2 r) r \, dr$$

$$= [p_1 J_1(p_1) J_0(p_2) - p_2 J_0(p_1) J_1(p_2)]/(p_1^2 - p_2^2), \qquad p_1 \neq p_2 \tag{31}$$

$$= \frac{1}{2}[J_0^2(p_1) + J_1^2(p_1)], \qquad p_1 = p_2 \tag{32}$$

where p_1 and p_2 are constants.

$$\int_0^1 J_1(p_1 r)J_1(p_2 r)r\,dr$$

$$= [p_2 J_1(p_1)J_0(p_2) - p_1 J_0(p_1)J_1(p_2)]/(p_1^2 - p_2^2), \qquad p_1 \neq p_2 \tag{33}$$

$$= \frac{1}{2}\left[J_0^2(p_1) - \frac{2}{p_1}J_0(p_1)J_1(p_1) + J_1^2(p_1)\right], \qquad p_1 = p_2. \tag{34}$$

The integrals involving the prescribed end conditions can be evaluated either in closed form or numerically, depending on the type of prescribed functions. The infinite set of equations are truncated for a given number of modes m and solved for the Fourier–Bessel coefficients.

It may be noted that if λ_j is an eigenvalue its conjugate $\bar{\lambda}_j$ is also an eigenvalue when c_i are real, and $\overline{K\lambda_j}$ is an eigenvalue when c_i are complex. For both the cases $\bar{F}_j$ is an eigenfunction where F_j corresponds to λ_j. Assuming that λ_j is complex and $F_{j+1} = \bar{F}_j$, it follows that $A_{pj+1} = \bar{A}_{pj}$, $p = 1, 2$, because the stresses and displacements are real. Since the eigenspectrum in general may consist of both real and complex roots it is computationally advantageous to carry out the solution of A_{pj} in real mode. While computing the elements of $[S_{kj}]$, whenever $F_{k+1} = \bar{F}_k$ it is enough to compute S_{kj}, $j = 1, \ldots m$, because S_{k+1j}, $j = 1, \ldots m$ can be easily derived from S_{kj}. Then, by noting that $A_{pk+1} = \bar{A}_{pk}$, $p = 1, 2$, one can obtain a real coefficient matrix instead of $[S_{kj}]$ and a real vector whose elements are A'_{pk} and A''_{pk} where $A_{pk} = (A'_{pk} + iA''_{pk})$. The coefficient matrix involved in the orthogonality technique turns out to be unsymmetric because of the nonself-adjoint nature of the basic eigenproblem.

Least-square technique

The boundary residuals at the ends may be minimized using the least-square procedure. The details of the method applied to a semi-infinite cylinder may be found in [5]. The least-square integrals of the boundary residuals can be compactly programmed using the integrals in eqns (31)–(34). The elements of the coefficient matrix, which is symmetric and positive definite, have been computed as described earlier. For additional comparison a least-square point matching technique has been used with composite Simpson's rule for numerical integration. Whenever the integrals involving the prescribed end conditions could not be evaluated analytically, the orthogonality as well as least-square integral techniques also used numerical integration for such integrals.

5. EXAMPLE PROBLEMS

The following problems are chosen for numerical study.

(a)
$$\bar{\sigma} = (1 - 2r^2)\bar{E}_m \quad \text{and} \quad \bar{\tau} = 0 \quad \text{at} \quad z = z_0$$
$$\bar{\sigma}' = \pm(1 - 2r^2)\bar{E}_m \quad \text{and} \quad \bar{\tau}' = 0 \quad \text{at} \quad z = -z_0 \tag{35}$$

(b)
$$\bar{w} = W \quad \text{and} \quad \bar{u} = \beta r \quad \text{at} \quad z = z_0$$
$$\bar{w}' = -W \quad \text{and} \quad \bar{u}' = \beta r \quad \text{at} \quad z = -z_0 \tag{36}$$

where W and β are constants. The end conditions (36) can be attained in a cylinder with rigidly bonded ends when a uniform temperature drop of T°C occurs. If α is the coefficient of linear expansion, $\bar{w} = \alpha T z_0$ and $\beta = \alpha T$. Another practically interesting case is a cylinder compressed between two rigid end plates. If the end plates are such as to constrain the inplane displacement, $\beta = 0$.

(c)
$$\bar{\sigma} = \bar{\tau} = 0 \quad \text{at} \quad z = z_0$$
$$\bar{w}' = \beta(1 - 2r^2) \quad \text{and} \quad \bar{\tau}' = 0 \quad \text{at} \quad z = -z_0. \tag{37}$$

The solution for the above end conditions together with the elementary solution of the cylinder under self-weight (ρ per unit volume) corresponds to a cylinder resting under its own weight on a smooth plane at $z = -z_0$. The expression for $\bar{w}'$ has been obtained from the elementary solution by prescribing $\int_0^1 wr\,dr = 0$ at $z = -z_0$. Two TI materials, namely, magnesium and a

Table 1. Material properties and eigenvalues for the TI cylinders*

Magnesium [5]	Hardwood
$a = 8.18\ E_m$, $(a-2\bar{\mu}) = 3.34\ E_m$, $b = 2.62\ E_m$	$a = 0.9365 \times 10^{-1}\ E_w$, $(a-2\bar{\mu}) = 0.4920 \times 10^{-1}\ E_w$
$\bar{a} = 8.5\ E_m$, $\mu = 2.44\ E_m$; $E_m = 1 \times 10^6$ psi	$b = 0.7143 \times 10^{-1}\ E_w$, $\bar{a} = 0.1071 \times 10^{-1}\ E_w$
$c_1^2 = 0.5269$ and $c_2^2 = 1.972$	$\mu = 0.6667 \times 10^{-1}\ E_w$; E_w is the axial modulus of elasticity
	$c_1^2 = 0.8912$ and $c_2^2 = 12.84$
λ_j	λ_j
$2.088 \pm i\ 0.7851$	1.071
3.550	$2.109 \pm i\ 0.2869$
$5.351 \pm i\ 0.6927$	2.481
6.839	3.486
$8.555 \pm i\ 0.6898$	4.382
10.13	$5.356 \pm i\ 0.2773$

*Although up to a maximum of 35 sets of eigenvalues were used in the calculations, only the first 6 sets are given here.

typical hardwood are used for numerical illustration. The material properties and the first six sets of eigenvalues for cylinders with stress-free lateral surfaces are given in Table 1. Note that the properties of magnesium are more nearly isotropic than those of hardwood.

6. RESULTS AND DISCUSSION

Cylinder with prescribed end stresses

The results for both the symmetric and antisymmetric cases (eqn 35) are shown in Figs. 1 and 2. For the symmetric case the convergence is excellent for the range of l/r_0 ratios considered ($z_0 = 3.0$–0.05). The accuracy for a given number of eigenfunctions m actually increased for lower values of l/r_0. However, the accuracy for antisymmetric cases deteriorates with decreasing l/r_0. For one particular case, with $l/r_0 = 0.2$ and $m = 53$, the end stress fit has a maximum error of 4% at $r = 1$ and considerably less error at other points. The superposition of the symmetric and antisymmetric end loadings results in a "thick plate" with a self-equilibrated loading of $\bar{\sigma} = 2(1-2r^2)\bar{E}_m$ on $z = z_0$. For this case, the results in Fig. 3 indicate that the normal stresses due to bending tend to become linear in z as the plate gets thinner, thus corroborating the Kirchhoff assumption for thin plates. A comparison of the plane stress solution for a thin plate with loads on both the ends, obtained from the analysis in Appendix 2, with the exact analysis indicates that the plane stress assumption gives sufficiently accurate results for $l/r_0 \leq 1/20$. A few typical results are shown in Fig. 4.

Cylinder with prescribed end displacements

The end conditions (36) are known to have a singularity at $r = 1$, $z = \pm z_0$, which will affect the convergence of the solution near the singular point. Accordingly the numerical results reveal an accurate displacement fit at the ends except near $r = 1$. Since the stresses are obtained from the displacements by differentiation, the numerical results for the stresses at the ends do not converge especially due to the presence of higher order eigenfunctions. However the convergence is found to be good at $z = \pm(z_0 - 0.1)$ as also observed in a semi-infinite case [5].

While prescribing an axial displacement uniformly over the end, if the u displacements at $\pm z_0$ are not constrained the solution obviously is given by the zero-eigenvalue solution in eqn (18). But when u is constrained at the ends a certain axial displacement is produced which when arrested gives rise to an additional axial force. For example, when a constrained magnesium cylinder (condition 36) undergoes an axial displacement of $\bar{w} = -\bar{w}' = -z_0/10^6$ at the ends the elementary solution gives $\sigma_{zz} = -7.3079\ \bar{E}_m$. Whereas the average σ_{zz} by the exact analysis depends on the l/r_0 ratio. For $l/r_0 = (3., 2., 1., 0.5)$ the average σ_{zz} are $-(7.375, 7.408, 7.513, 7.738) \times \bar{E}_m$. For the hardwood cylinder the corresponding values are $-(1.006, 1.010, 1.020, 1.037) \times \bar{E}_w$ whereas by the elementary solution $\sigma_{zz} = -1.0 \times \bar{E}_w$. The axial stress variations are plotted in Fig. 5. The ratios of normal to shear stresses in the end zone suggest that for a

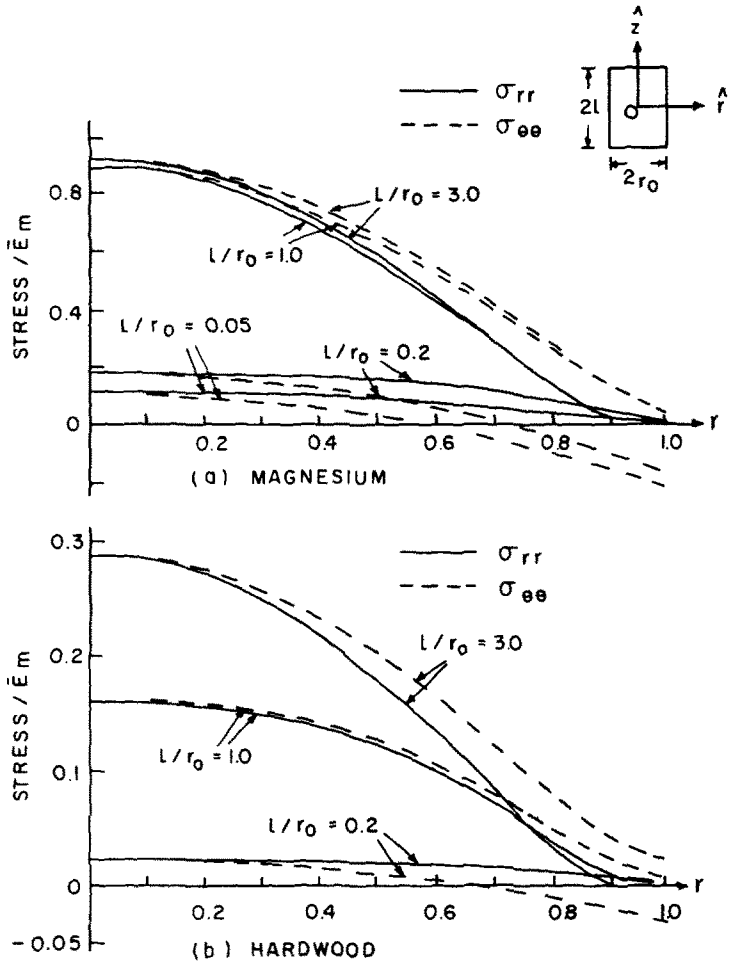

Fig. 1. Stresses in finite cylinders under $\bar{\sigma} = \bar{\sigma}' = (1-2r^2)\bar{E}_m$ and $\bar{\tau} = \bar{\tau}' = 0$; $\bar{E}_m = E_m/10^6$.

cylinder compressed between end plates a full restraint on u seems practically feasible if sufficient friction exists. Although the effect of such a constraint is not quite significant for the example materials, it has been found to be appreciable in the case of elastomeric cylinders[10]. For a constrained cylinder undergoing a uniform temperature drop the results are given in Fig. 6. The increase in the average σ_{zz} with decreasing l/r_0 ratio, observed in both the above problems, may be ascribed to the fact that the axial displacement caused by the constraint on u produces a larger axial force in a shorter cylinder.

Cylinder under self-weight

The end conditions (37) illustrate a combination of purely stress conditions at one end and a mix of stress and displacement conditions at the other. The mixed conditions at $z = -z_0$ lead to closed-form expressions for the Fourier–Bessel coefficients for a semi-infinite case. For a finite cylinder, the orthogonality equation at $z = -z_0$ is used to eliminate A_{2k} in eqn (24) thus resulting in a reduced problem size. The axial stresses for a cylinder resting under its own weight with $l/r_0 = 0.5$ are displayed in Fig. 7.

For sufficiently large values of l/r_0, the end conditions (37) tend to represent a semi-infinite cylinder with mixed end conditions at $z = -z_0$. The results for this case are shown in Fig. 8.

Least-square procedure

The least-square integral procedure has been used to solve a semi-infinite cylinder with stress as well as displacement end conditions. The results reveal a slightly more accurate boundary fit compared to the orthogonality technique. The computation times for the two methods did not differ significantly. The least-square point matching technique with $m = 38$ and

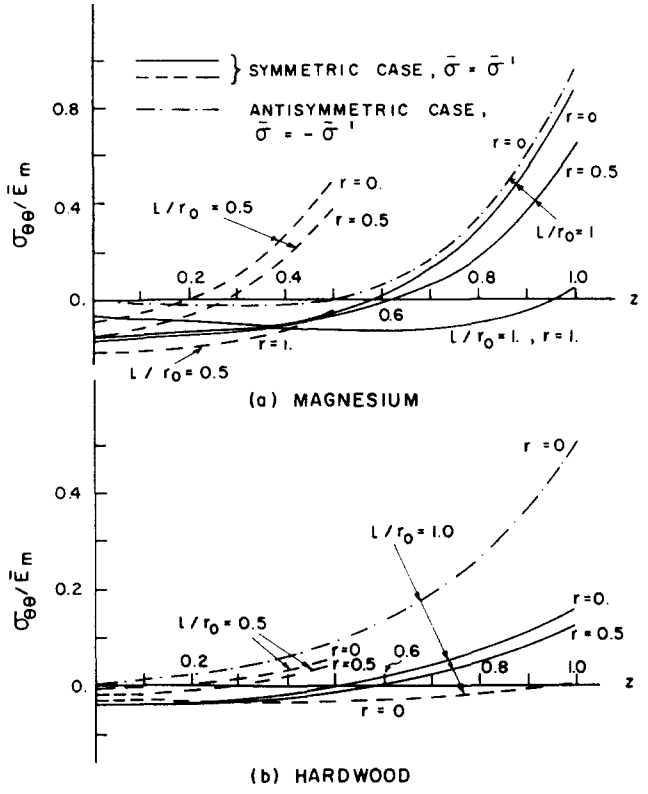

Fig. 2. Stresses in finite cylinders under $\bar{\sigma} = (1 - 2r^2)\bar{E}_m$, $\bar{\sigma}' = \pm\bar{\sigma}$ and $\bar{\tau} = \bar{\tau}' = 0$.

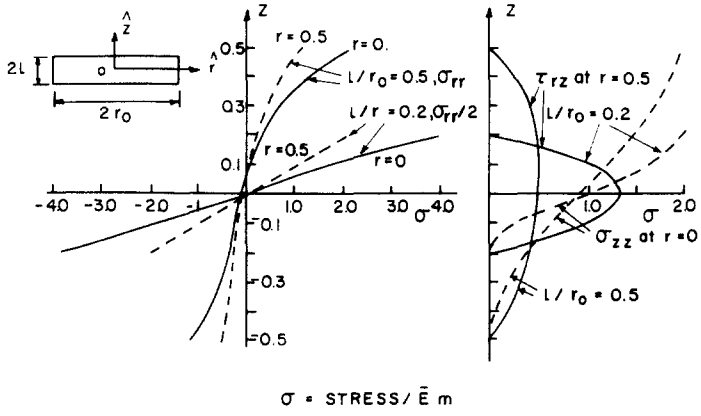

Fig. 3. Stresses in thick plates under $\bar{\sigma} = 2(1 - 2r^2)\bar{E}_m$ and $\bar{\sigma}' = \tau = \bar{\tau}' = 0$—magnesium.

with 30 subdivisions for numerical quadrature yielded results of sufficient accuracy, although the computation time increased substantially.

7. CONCLUSIONS

The exact analysis of transversely isotropic axisymmetric finite cylinders has been considered using a displacement potential formulation. The solution was expressed as an aggregate of the radial eigenfunctions which satisfy the lateral boundary conditions. The Fourier–Bessel coefficients of the expansion have been evaluated using the general orthogonality relations among the eigenfunctions. The orthogonality technique has been applied to typical cases of stress, displacement as well as mixed end conditions. The method lends itself to easy programming for a digital computer. The least-square integral as well as point matching

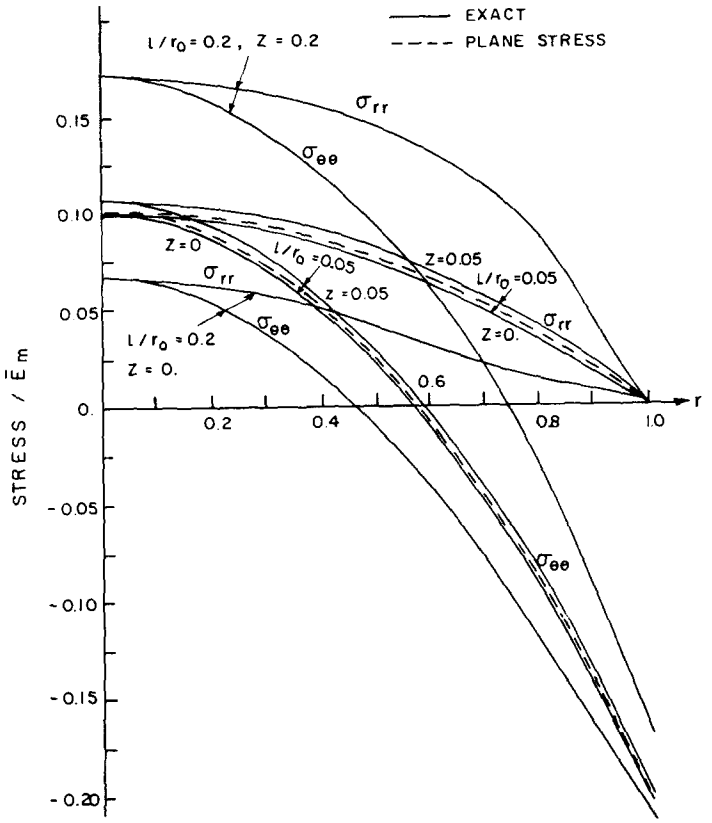

Fig. 4. Exact and plane stress solutions for finite cylinders under $\bar{\sigma} = \bar{\sigma}' = (1-2r^2)\bar{E}_m$ and $\bar{\tau} = \bar{\tau}' = 0$—magnesium.

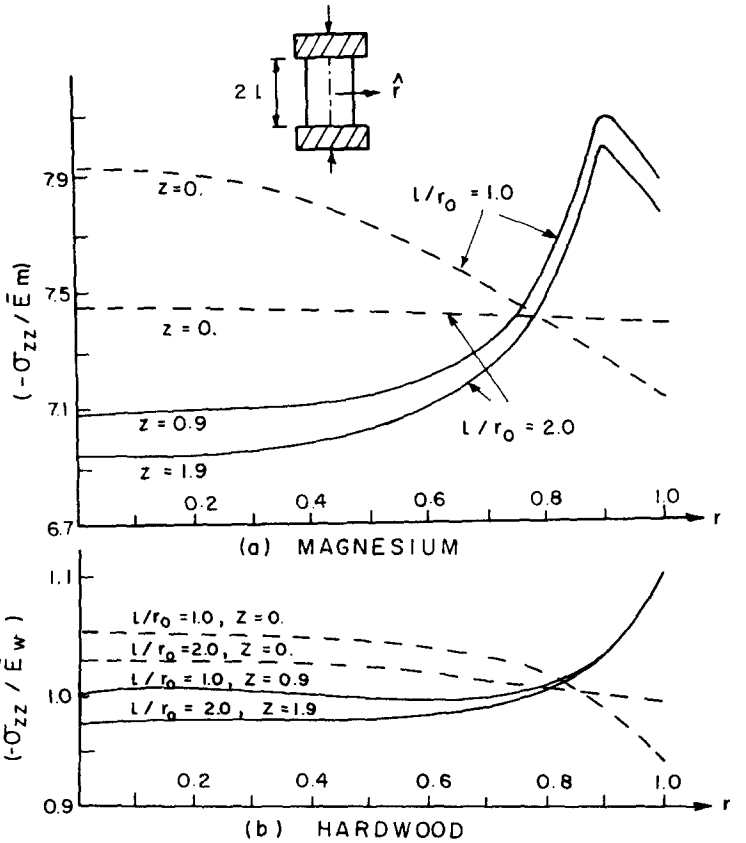

Fig. 5. Axial stresses in cylinders compressed between two plates bonded to the ends $\bar{w} = -\bar{w}' = -(l/r_0)/10^6$ and $\bar{u} = \bar{u}' = 0$; $\bar{E}_{m,w} = E_{m,w}/10^6$.

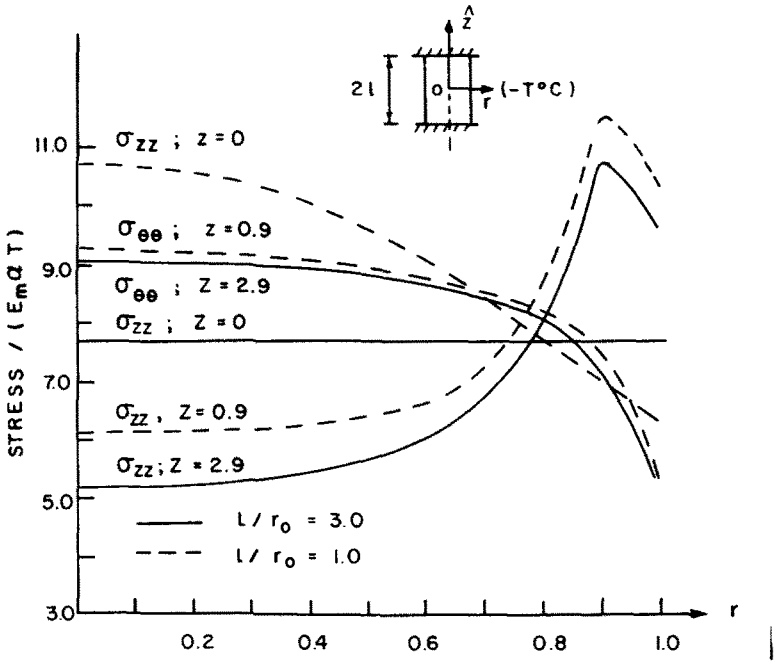

Fig. 6. Stresses in a constrained magnesium cylinder due to uniform temperature drop.

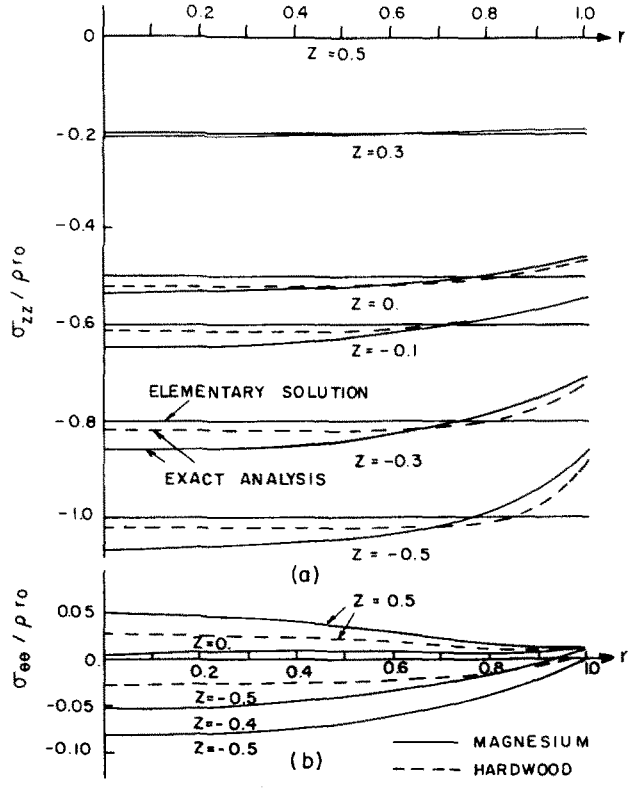

Fig. 7. Axial and circumferential stresses in a cylinder under self-weight $-l/r_0 = 0.5$.

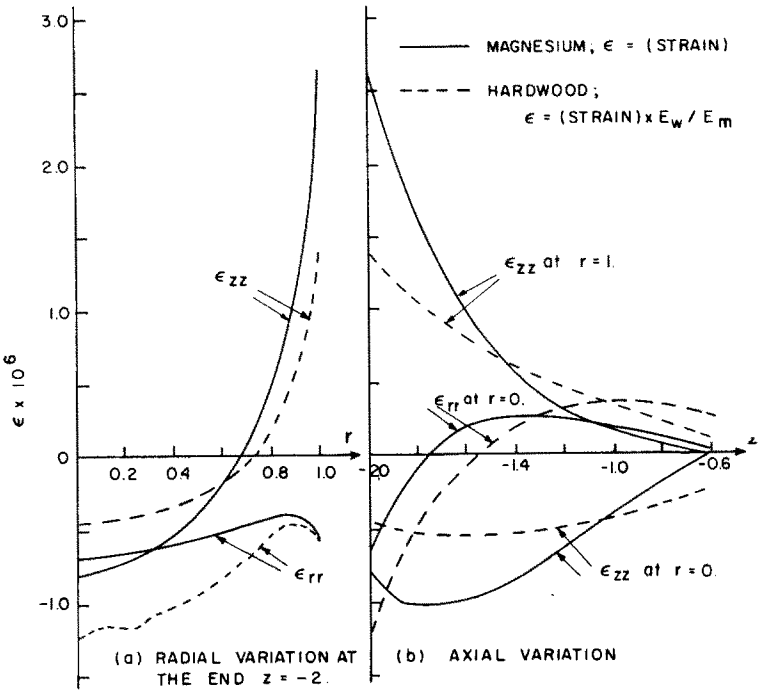

Fig. 8. Strains in semi-infinite cylinders under $\bar{w}' = (1 - 2r^2)/10^6$ and $\bar{r}' = 0$ at end $z = -2$.

techniques were also considered. Comparison of a few results by the least-square integral method with those from the orthogonality technique revealed that the former method yielded a slightly more accurate boundary fit than the later method. The computation times for the two methods did not differ significantly in these cases. However, for problems with mixed end conditions the orthogonality technique involves a reduced problem size. The least-square point matching technique was found to yield sufficiently accurate results although it involved substantially more computation time.

REFERENCES

1. A. I. Luré, *Three-Dimensional Problems of the Theory of Elasticity* (Translated by D. B. McVean), pp. 428–439.Interscience, New York (1964).
2. G. W. Swan, The semi-infinite cylinder with prescribed end displacements. *SIAM J. Appl. Math.* **16**, 860–881 (1968).
3. J. L. Klemm and R. W. Little, The semi-infinite elastic cylinder under self-equilibrated loading. *SIAM, J. Appl. Math.* **19**, 712–729 (1970).
4. J. L. Klemm and R. W. Little, Saint-Venant Principle, *Tech. Rep.* No. 10.1, 79 pp, Division of Engineering Research, Michigan State University, East Lansing (1971).
5. W. E. Warren, A. L. Roark and W. E. Bickford, The end effect in semi-infinite transversely isotropic cylinders. *A.I.A.A. J.* **5**, 1448–1455 (1967).
6. R. W. Little and S. B. Childs, Elastostatic boundary region in solid cylinders. *Quart. Appl. Math.* **25**, 261–274 (1967).
7. M. E. D. Fama, Radial eigenfunctions for the elastic circular cylinder. *Quart. J. Mech. Appl. Math.*, Vol. 25, 479–495 (1972).
8. F. E. Byrnes and R. R. Archer, Orthogonality relations for the "end problems" for transversely isotropic cylinders. *A.I.A.A. J.* **13**, 357–360 (1975).
9. G. Pickett, Application of the fourier method to the solution of certain boundary problems in the theory of elasticity. *J. Appl. Mech.* **11**, A176–182 (1944).
10. S. R. Moghe and H. F. Neff, Elastic deformations of constrained cylinders. *J. Appl. Mech.* **38**, 393–399 (1971).
11. L. D. Power and S. B. Childs, Axisymmetric stresses and displacements in a finite circular bar. *Int. J. Engng Sci.* **9**, 241–255 (1971).
12. D. N. Mitra, On axisymmetric deformations of transversely isotropic elastic circular cylinder of finite length. *Archiwum Mechaniki Stosowanej*, **17**, 739–749 (1965).
13. R. A. Eubanks and E. Sternberg, On the axisymmetric problem of elasticity for a medium with transverse isotropy. *J. Rat. Mech. Anal.* **3**, 89–101 (1954).
14. J. L. Beck, Anisotropic theory of growth stresses in trees, Rep. No. 452, 32 pp. Department of Scientific and Industrial Research, Lower Hutt, New Zealand, (1974).
15. H. T. Davis, *The Theory of Linear Operators*, pp. 130–133. Principia Press, New York (1936).

APPENDIX 1

The series in eqn (21) converges provided the eigenfunctions F_j (eqn 14) are complete. The completeness of the eigenfunctions for the case of a cylinder with stress-free lateral surface is yet to be proved[7]. However the convergence of the numerical results from many investigations suggest that the eigenfunctions may be complete in the appropriate space. The following discussion is concerned with the question whether the sequence of solutions obtained by truncating the infinite system (30) converges to a limit. Let

$$\langle A_{1k}^{(m)}, A_{2k}^{(m)}\rangle, \quad k = 1, 2 \ldots m$$

be the solution of eqn (30) for m eigenfunctions in eqn (21). The sequence of solutions $\{\langle A_{1k}^{(m)}, A_{2k}^{(m)}\rangle\}$ converge to a limit as $m \to \infty$ if in eqn (30)

$$\sum_{q=1}^{\infty} |S_{pq}| < \infty, \qquad p = 1, 2, \ldots \infty \tag{A1}$$

and the elements of $\{P\}$ are bounded[15].

An analytical investigation of the condition (A.1) will not be attempted here. Instead, the numerical form of the coefficient matrix for a given set of end conditions will be used to verify the convergence condition. The real coefficient matrix (discussed in Section 4) is computed for two cases, one with stress and the other with displacement end conditions. A maximum value of $m = 47$ has been considered. The absolute sum, as defined in eqn (A1), of the first row of the matrix converges to the fourth significant digit. The next few rows show convergence to the third significant digit. A definite tendency of numerical convergence could be observed up to about forty rows although the summation was carried up to only 47 terms. Thus it appears that the sequence of solutions obtained by truncating the infinite system in eqn (30) may converge to a limit. This observation together with the observed convergence of the results for stresses and displacements suggest that the eigenfunctions may be complete.

APPENDIX 2

Plane stress analysis of a thin TI *disc*

Consider an axisymmetric cylinder with the end conditions $\sigma_{zz} = \bar{\sigma}(r)$ and $\tau_{rz} = 0$ at $z = \pm z_0$. For a thin disc a plane stress state may be assumed:

$$\left.\begin{aligned} \sigma_{zz} &= \bar{\sigma} \\ \tau_{rz} &= 0 \end{aligned}\right\} \quad \text{for all } z. \tag{B1}$$

Then from the stress–strain relation for σ_{zz} one has

$$\epsilon_{zz} = [\bar{\sigma} - b(\epsilon_{rr} + \epsilon_{\theta\theta})]/\bar{a}. \tag{B2}$$

In view of eqn (B1) the axial equilibrium equation is identically satisfied. Then, using the stress–strain relations and eqn (B2), the radial equilibrium equation in terms of u becomes

$$r^2 \frac{d^2u}{dr^2} + r\frac{du}{dr} - u = -\{br^2/(a\bar{a} - b^2)\}\frac{d\bar{\sigma}}{dr}. \tag{B3}$$

Beck[14] used a similar analysis for a thin orthotropic disc. Let $\bar{\sigma} = (1 - 2r^2)\bar{E}_m$. Then the solution of eqn (B.3) may be written as

$$u = Cr + Dr^3 \tag{B4}$$

where

$$D = \bar{E}_m P/8, \quad P = -4b/(a\bar{a} - b^2)$$

$$C = \bar{E}_m\{b/\bar{a} - P(3R + S)/8\}/(R + S)$$

$$R = (a - b^2/\bar{a}), \qquad S = (a - 2\bar{\mu}) - b^2/\bar{a}.$$

The other displacement and stresses can be readily evaluated using the expressions for ϵ_{zz} and u.